Research internship

Notes on project in DiVincenzo group

Jesse Slim

January 16, 2018

Abstract

Magnus expansion

Contents

1. Impulse operators

The effective Hamiltonian generated from the Magnus expansion is applicable if the driving envelope is varied analytically. However, if the driving envelope experiences a non-analytical change, such as a sudden turn-on, an extra "impulse operator" is needed to describe the "jump" between the effective trajectory before and after the change. In this section we will work towards the development of such impulse operators.

1.1. Piecewise analytical driving envelopes

We start with a two-level system that is driven by a perpendicular ($\boldsymbol{\sigma}_x$) oscillating signal of frequency ω with a slowly (compared to ω) varying envelope $E(t)$. In the frame that rotates along with the driving frequency ω, the Hamiltonian of the driven system is given by

$$\begin{aligned}\boldsymbol{H}_{\text{real}}(t) &= \frac{E(t)}{4}\left(\cos(\phi)\boldsymbol{\sigma}_x + \sin(\phi)\boldsymbol{\sigma}_y + \cos(2\omega t+\phi)\boldsymbol{\sigma}_x - \sin(2\omega t+\phi)\boldsymbol{\sigma}_y\right) + \frac{\Delta}{2}\boldsymbol{\sigma}_z \\ &= E(t)\boldsymbol{H}_p(t) + \frac{\Delta}{2}\boldsymbol{\sigma}_z, \end{aligned} \tag{1}$$

where we define $\boldsymbol{H}_p(t)$ as the periodic part of the Hamiltonian.

As detailed in Daniel's notes, we can use the Magnus expansion to construct an effective evolution operator that coincides stroboscopically with the actual evolution operator. In this construction, the Hamiltonian (1) and higher-order commutators are integrated over an interval $[t_0, t_0 + t_c]$, with $t_c = \pi/\omega$ corresponding to the period of $\boldsymbol{H}_p(t)$. In addition, to facilitate the integration of eq. (1), the envelope function $E(t)$ is replaced by a Taylor series around t_0. Therefore, to accurately capture the behaviour of the system, the envelope function must be approximated reasonably well by its Taylor series on the interval $[t_0, t_0 + t_c]$. If a non-analyticity occurs within this interval, this is obviously not the case.

Figure 1 illustrates this situation. A system, initially in the state $|\psi_{\text{real}}(t=0)\rangle = |0\rangle$, is driven using a particular driving envelope, shown in Figure 1(a), that exhibits discontinuities at the turn-on time $t = 0$ and the turn-off time t_d, in addition to a discontinuity at $t_j = t_d/2$. For this discussion, we focus on the discontinuity at t_j and define $E_l(t)$ ($E_r(t)$) as the part of the envelope function to the left (right) of t_j.

Our goal now is to find an effective trajectory $|\psi_{\text{eff}}(t)\rangle$ that (a) stroboscopically coincides with the actual trajectory, and (b) evolves corresponding to $E_l(t)$ for $t < t_j$ and to $E_r(t)$ for $t > t_j$. The second condition fixes the shape of the effective trajectory sections $|\psi_{\text{eff}}(t)\rangle_l$ and $|\psi_{\text{eff}}(t)\rangle_r$ to the left and right of t_j, while the first condition fixes the positions of these sections. Although the real trajectory is necessarily continuous everywhere under unitary evolution, in general, the combined effective trajectory is not continuous at t_j, as shown in Figure 1(b). We describe this discontinuity with an "impulse operator", which will be subject of the next section.

1.2. The impulse operator

The impulse operator Ω_j is defined as the generator of the unitary operator that rotates the endpoint $|\psi_{\text{eff}}(t_j)\rangle_l$ of the effective trajectory section to the left of t_j to the starting point $|\psi_{\text{eff}}(t_j)\rangle_r$ of the section to the right of t_j. That is,

$$|\psi_{\text{eff}}(t_j)\rangle_r = e^{\Omega_j}\,|\psi_{\text{eff}}(t_j)\rangle_l\,. \tag{2}$$

From Figure 1(b), we see that

$$e^{\Omega_j} = (e^{\Omega_D})^{-1} e^{\Omega_C} (e^{\Omega_B})^{-1} e^{\Omega_A} = e^{-\Omega_D} e^{\Omega_C} e^{-\Omega_B} e^{\Omega_A}, \tag{3}$$

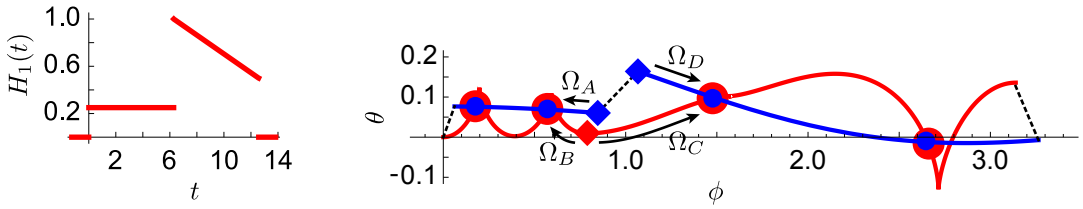

(a) | Piecewise analytical drive. **(b)** | Trajectories.

Figure 1 | Effective Magnus trajectories under a piecewise analytical driving envelope. (a) | An exemplary piecewise analytical driving envelope is shown. This envelope, with a total pulse duration of $t_d = 12.57$, exhibits non-analyticities at $t = 0$ (turn-on time), $t = t_d/2$ and $t = t_d$ (turn-off time). The average drive strength over the total pulse duration is $\overline{H}_1 = 0.5$, such that the rotation induced by driving a two-level system with this particular pulse is $\theta_d = \overline{H}_1 t_d/2 = \pi$ in the rotating wave approximation. **(b)** | The axes on this figure represent the spherical latitude θ and longitude ϕ on a rotated Bloch sphere, i.e. a Bloch sphere that has the state $|+\rangle$ as its north pole. In particular, $\theta = 2\arccos\left(|\langle\psi|+\rangle|\right) - \pi/2$ and $\phi = \arg\left(\langle\psi|-\rangle\right) - \arg\left(\langle\psi|+\rangle\right)$. The evolution (red line) of a system initially in the $|0\rangle$ state, driven by a sinusoidal signal with an envelope as given in Figure (a), is obtained through numerical integration. In addition, the stroboscopic Magnus trajectory of order $1/\omega^2$ (blue lines) is plotted. The actual and stroboscopic trajectories approximately coincide every $t_c = \pi/\omega$, starting at $t_0 = \alpha_0/\omega$ (red, blue dots). At each non-analytical point in the driving envelope, the stroboscopic trajectory shows a "jump" (dashed lines). For the second discontinuity, at $t = t_d/2$, the corresponding point on each trajectory is indicated (diamond). Around this discontinuity, generators of evolution operators along several sections of the actual and the stroboscopic trajectories are marked (Ω_i) and expanded upon in the main text. Relevant parameters are $\omega = 1$, $\alpha_0 = 0.9$.

where $\Omega_i, i \in \{A, B, C, D\}$ are all generators of unitaries that describe the evolution between certain points on the actual and effective trajectories. In particular,

$$|\psi_{\text{eff}}(t_0)\rangle_l = e^{\Omega_A} |\psi_{\text{eff}}(t_j)\rangle_l \tag{4}$$

$$|\psi_{\text{real}}(t_0)\rangle = e^{\Omega_B} |\psi_{\text{real}}(t_j)\rangle \tag{5}$$

$$|\psi_{\text{real}}(t_0 + t_c)\rangle = e^{\Omega_C} |\psi_{\text{real}}(t_j)\rangle \tag{6}$$

$$|\psi_{\text{eff}}(t_0 + t_c)\rangle_r = e^{\Omega_D} |\psi_{\text{eff}}(t_j)\rangle_r \,. \tag{7}$$

The definition of the effective trajectory requires that $|\psi_{\text{eff}}(t_0)\rangle_l = |\psi_{\text{real}}(t_0)\rangle$ and $|\psi_{\text{eff}}(t_0 + t_c)\rangle_r = |\psi_{\text{real}}(t_0 + t_c)\rangle$. Equation (3) then follows immediately from definitions (4)-(7) and the stroboscopic coincidence condition.

We use explicit Magnus expansions (as per Daniel's definition) to express the four Ω_i's. For example,

$$\Omega_A = M\left[H_{\text{eff},l}(t), t_0, t_j\right]. \tag{8}$$

For this particular explicit Magnus expansion, we substitute $E(t)$ by a Taylor expansion of $E_l(t)$ around t_j. For the other explicit Magnus expansions we also substitute $E(t)$ by a Taylor expansion around t_j of $E_l(t)$ or $E_r(t)$ appropriately. Finally, we construct an expression for Ω_j by repeated application of the Baker-Campbell-Hausdorff (BCH) formula to equation (3).

1.3. The impulse operator as a power series in $1/\omega$

In principle, the impulse operator introduced in the previous section is exact if the relevant Magnus and Taylor expansions and the BCH formula are treated up to infinite order. In this section we will

discuss how to calculate the impulse operator up to finite order k in $1/\omega$.

As a first step, we express the two relevant times in the problem, t_0 and t_j, relative to the time scale $1/\omega$ of the power series by introducing the angle-like quantities $\alpha_0 = \omega t_0$ and $\alpha_j = \omega t_j$. We then calculate explicit Magnus expansions for all four Ω_i's (cf. eq. (8)) up to the desired order k in $1/\omega$, using the method detailed in Daniel's notes. Noting that the impulse operator needs to be dimensionless, a similar dimensional argument as applied in Daniel's note leads us to the conclusion that the highest relevant order of the envelope Taylor expansions is $k-1$.

Subsequently, we note that the substitutions $t_0 = \alpha_0/\omega$ and $t_j = \alpha_j/\omega$ render all integral bounds in the Magnus expansion proportional to $1/\omega$, such that the integrals and therefore the Ω_i's themselves become proportional to $1/\omega$. This implies that an n-th order nested commutator of Ω_i's is proportional to $1/\omega^{n+1}$. Therefore, the highest order of nested commutators in the BCH formula we need to take into account is $k-1$.

After putting this machinery to work, we arrive at a power series for the impulse operator Ω_j. The first three terms are given by

$$\Omega_j = \sum_{i=0}^{\infty} \frac{1}{\omega^i} \Omega_j^{(i)}, \tag{9}$$

$$\Omega_j^{(0)} = 0, \tag{10}$$

$$\Omega_j^{(1)} = i\frac{\sin(\alpha_j - \alpha_0)}{4}(E_r - E_l) \cdot (\cos(\phi + \alpha_0 + \alpha_j)\boldsymbol{\sigma}_x - \sin(\phi + \alpha_0 + \alpha_j)\boldsymbol{\sigma}_y), \tag{11}$$

$$\begin{aligned}\Omega_j^{(2)} = & -i\frac{\sin(\alpha_j - \alpha_0)}{32} \times \\ & \Big(4\Delta(E_r - E_l) \cdot \big(\cos(\phi + \alpha_0 + \alpha_j)\boldsymbol{\sigma}_x + \sin(\phi + \alpha_0 + \alpha_j)\boldsymbol{\sigma}_y\big) \\ & + 4(\dot{E}_r - \dot{E}_l) \cdot \big(\sin(\phi + \alpha_0 + \alpha_j)\boldsymbol{\sigma}_x - \cos(\phi + \alpha_0 + \alpha_j)\boldsymbol{\sigma}_y\big) \\ & + (E_r^2 - E_l^2) \cdot \big(\cos(\alpha_j - \alpha_0) - 2\cos(2\phi + \alpha_0 + \alpha_j)\big)\boldsymbol{\sigma}_z\Big),\end{aligned} \tag{12}$$

where $E_{r,l}$ and $\dot{E}_{r,l}$ are shorthand for the Taylor coefficients $E_{r,l}(t_j)$ and $\dot{E}_{r,l}(t_j)$ respectively.

1.3.1 Final and initial impulse operators

The impulse operator formalism is also capable of describing the discontinuity in the effective trajectory during a non-analytical turn-on or turn-off of the driving field. In this case, either $E_l(t)$ or $E_r(t)$ is identically zero and the expressions (10)-(12) simplify accordingly.

In addition, for computational simplicity when calculating higher order initial or final impulse operators, we can simplify eq. (3) considerably. For example, if we're interested in the turn-on discontinuity at $t = 0$, for $t < 0$ the system Hamiltonian is given by

$$\boldsymbol{H}_{\text{real}}(t) = \frac{\Delta}{2}\boldsymbol{\sigma}_z. \tag{13}$$

This Hamiltonian is constant and can be represented exactly in the effective Hamiltonian formalism, even at the lowest (zeroeth) order in $1/\omega$. Therefore, we can take $\boldsymbol{H}_{\text{eff}}(t) = \boldsymbol{H}_{\text{real}}(t)$ for $t < 0$. Then it follows that $\Omega_A = -i\boldsymbol{H}_{\text{eff}}(t_0 - t_j) = -i\boldsymbol{H}_{\text{real}}(t_0 - t_j) = \Omega_B$ and

$$e^{\Omega_j} = e^{-\Omega_D} e^{\Omega_C}. \tag{14}$$

A similar argument can be made for the turn-off discontinuity. Note that the "turn-off impulse operator" can also be used at any point in time t to calculate the transformation from the effective trajectory to the real trajectory at that time.

2. The truncated Magnus expansion

The Magnus expansion[1–4] for the time evolution under Hamiltonian $H(t)$ is defined as

$$\Omega(t,t_0) = \sum_{n=1}^{\infty} \Omega_n(t,t_0), \tag{15}$$

$$\Omega_1(t,t_0) = \int_{t_0}^{t} \mathrm{d}t_1 \tilde{H}(t_1), \tag{16}$$

$$\Omega_2(t,t_0) = -\frac{1}{2}\int_{t_0}^{t} \mathrm{d}t_1 \left[\Omega_1(t_1,t_0), \tilde{H}(t_1)\right] = \frac{1}{2}\int_{t_0}^{t} \mathrm{d}t_1 \int_{t_0}^{t_1} \mathrm{d}t_2 \left[\tilde{H}(t_1), \tilde{H}(t_2)\right], \tag{17}$$

where $\tilde{H}(t) = -i/\hbar H(t)$. In the remainder of these notes, natural units with $\hbar = 1$ will be used.

We use this series to approximate the trajectory of a two-level qubit driven by an oscillating signal proportional to $\boldsymbol{\sigma}_x$ in the lab frame. To this end, we use the following rotating frame Hamiltonian:

$$\boldsymbol{H}(t) = \frac{E(t)}{4}\left(\boldsymbol{\sigma}_x + \cos(2\omega t)\boldsymbol{\sigma}_x - \sin(2\omega t)\boldsymbol{\sigma}_y\right), \tag{18}$$

where for now we have set the detuning Δ and phase offset ϕ of the drive both to zero.

2.1. First order Magnus expansion

Initially, we restrict ourselves to the first order Magnus term, which is equivalent to the rotating wave approximation for constant drive. We begin by studying the case of linear drive, given by

$$E(t) = E_0 + E_1 t. \tag{19}$$

We then integrate equation (16) over a full period $t_c = \pi/\omega$ of the drive Hamiltonian (18), starting from t_0:

$$\begin{aligned}
i\Omega_1(t_0+t_c,t_0) =& \int_{t_0}^{t_0+t_c} \frac{E(t)}{4}\left(\boldsymbol{\sigma}_x + \cos(2\omega t)\boldsymbol{\sigma}_x - \sin(2\omega t)\boldsymbol{\sigma}_y\right)\mathrm{d}t \\
=& \int_{t_0}^{t_0+t_c} \frac{E(t)}{4}\boldsymbol{\sigma}_x\,\mathrm{d}t + \int_{t_0}^{t_0+t_c} \frac{E(t)}{4}(\cos(2\omega t)\boldsymbol{\sigma}_x - \sin(2\omega t)\boldsymbol{\sigma}_y)\,\mathrm{d}t \\
=& \frac{E_0 t_c + E_1(t_0 t_c + t_c^2/2)}{4}\boldsymbol{\sigma}_x + \frac{E_1 t_c \sin(2\omega t_0)}{8\omega}\boldsymbol{\sigma}_x + \frac{E_1 t_c \cos(2\omega t_0)}{8\omega}\boldsymbol{\sigma}_y \\
=& t_c\frac{E_0 + E_1 t_0}{4}\boldsymbol{\sigma}_x + t_c^2\frac{E_1}{8}\boldsymbol{\sigma}_x + \frac{t_c}{\omega}\left(\frac{E_1\sin(2\omega t_0)}{8}\boldsymbol{\sigma}_x + \frac{E_1\cos(2\omega t_0)}{8}\boldsymbol{\sigma}_y\right) \\
=& t_c\left[\frac{E_0 + E_1 t_0}{4}\boldsymbol{\sigma}_x + \frac{E_1}{8\omega}\left(\pi\boldsymbol{\sigma}_x + \sin(2\omega t_0)\boldsymbol{\sigma}_x + \cos(2\omega t_0)\boldsymbol{\sigma}_y\right)\right]
\end{aligned} \tag{20}$$

The first term of this evolution operator exponent,

$$t_c\frac{E_0 + E_1 t_0}{4}\boldsymbol{\sigma}_x = t_c\frac{E(t_0)}{4}\boldsymbol{\sigma}_x, \tag{21}$$

can be understood as the rotating wave evolution over a period t_c with constant drive given by the value of the driving envelope at the beginning of the evolution period $E(t_0)$. The second term,

$$t_c^2\frac{E_1}{8}\boldsymbol{\sigma}_x = t_c\frac{\pi E_1}{8\omega}\boldsymbol{\sigma}_x, \tag{22}$$

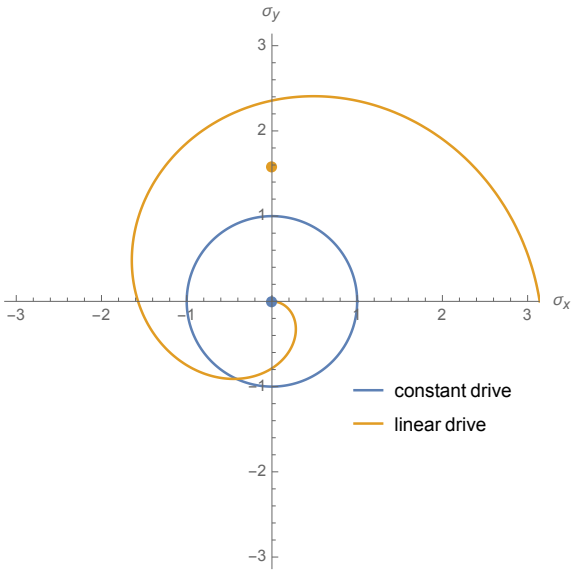

Figure 2 | Effect of the counter-rotating wave in the first order Magnus expansion. The $\boldsymbol{\sigma}_x$ and $\boldsymbol{\sigma}_y$ projections of the counter-rotating wave contribution, $E(t)\left[\cos(2\omega t)\boldsymbol{\sigma}_x + \sin(2\omega t)\boldsymbol{\sigma}_y\right]$, are traced for $t \in [t_0, t_0 + t_c]$ with $t_0 = 0$. Trajectories are shown both for constant drive $E(t) = 1$ and for a linearly increasing drive $E(t) = (t - t_0)$. The average projections are indicated with a dot. For constant drive, it can be seen that the average projection is zero, while for linear drive, the average is non-zero and directed $\pi/2$ radians from the initial (and final) projection. Choosing a different t_0 has the effect of rotating the trajectories and still leaves a non-zero average of equal magnitude in the linear drive case.

can still be understood in the rotating wave picture as the extra rotation brought about by the (linear) increase in driving strength during the evolution interval t_c. Keeping in mind that $t_c = \pi/\omega$, the effect of this term decreases if ω increases; i.e. the driving signal has less time to increase within one evolution interval.

The final two terms in equation (20),

$$t_c \frac{E_1}{8\omega} \left(\sin(2\omega t_0)\boldsymbol{\sigma}_x + \cos(2\omega t_0)\boldsymbol{\sigma}_y\right), \tag{23}$$

can no longer be understood in the rotating wave approximation. These terms constitute an average of the effect of the counter-rotating wave over a single evolution interval t_c, which is exactly the period of the counter-rotating wave. In the case of constant drive, i.e. $E_1 = 0$, this effect averages out to zero, but if the drive increases during the evolution interval, a non-zero average is obtained. The resulting "average counter-wave rotation axis" lies in the $x - y$ plane and has a constant magnitude, while the direction is determined by the start of the evolution interval t_0, as illustrated in Figure 2.

2.1.1 Effective Hamiltonian

Let's see if we can find an effective Hamiltonian that corresponds to (20). Per the procedure described in Daniel's notes, we proceed order by order of $1/\omega$, such that $H_{eff}^{(m)} = \sum_{n=0}^{m} (1/\omega)^n h_n$, where each h_n may not depend explicitly on t or ω and occurences of t_0 in (derivatives of) $H_1(t_0)$ are promoted to the instantaneous time t. We start with the trivial order $1/\omega^0 = 1$. In this case,

h_0 is given by

$$h_0 = \left[\frac{E(t_0)}{4}\boldsymbol{\sigma}_x\right]_{t_0\to t} = \frac{H(t)}{4}\boldsymbol{\sigma}_x. \tag{24}$$

For the next order $1/\omega^1$ we use the iterative relation

$$h_{n+1} = C[\bar{H}(t_0), 1/\omega, n+1] - C[\bar{H}^{(n)}_{eff}(t_0), 1/\omega, n+1]. \tag{25}$$

The first term is readily extracted from (20) and equal to

$$C[\bar{H}(t_0), 1/\omega, 1] = \frac{E_1}{8\omega}\left(\pi\boldsymbol{\sigma}_x + \sin(2\omega t_0)\boldsymbol{\sigma}_x + \cos(2\omega t_0)\boldsymbol{\sigma}_y\right). \tag{26}$$

The second term is obtained by calculating the Magnus expansion of (24) up to first order in $1/\omega$. Noting that h_0 is proportional to $\boldsymbol{\sigma}_x$ for all times and $[h_0(t_1), h_0(t_2)] = 0$ for all t_1, t_2, the first order Magnus expansion is exact and given by

$$\bar{H}^{(0)}_{eff}(t_0) = \left[\frac{E(t_0)}{4} + \frac{E_1}{8\omega}\pi\right]\boldsymbol{\sigma}_x. \tag{27}$$

Therefore,

$$C[\bar{H}^{(0)}_{eff}(t_0), 1/\omega, 1] = \frac{E_1}{8\omega}\pi\boldsymbol{\sigma}_x, \tag{28}$$

leaving us with

$$h_1 = \frac{E_1}{8\omega}\left(\sin(2\omega t_0)\boldsymbol{\sigma}_x + \cos(2\omega t_0)\boldsymbol{\sigma}_y\right). \tag{29}$$

Let's see if taking the Magnus expansion of this effective Hamiltonian indeed matches the ME of the real Hamiltonian over an interval t_c. As per the notebook 'linear_drive_manual_integration.nb' it does, up to first order! There is however a third order term (and higher order terms) that explains the deviation of the trajectory of the effective Hamiltonian from the stroboscopic evolution given by repeated application of $\exp[-it_c\bar{H}(t_0+kt_c)]$ with increasing k, as observed in numerical simulations for large driving strengths.

2.2. Second order Magnus expansion

We now continue by investigating the second order term in the Magnus expansion, given by (17), to gain some intuition. We first focus on rewriting the commutator in the integrand:

$$\begin{aligned}
&\frac{1}{2}\left[\tilde{H}(t_1), \tilde{H}(t_2)\right] = \frac{1}{2}\left[-iH(t_1), -iH(t_2)\right] = -\frac{1}{2}\left[H(t_1), H(t_2)\right] \\
&= -\frac{E(t_1)E(t_2)}{32}\left[\left((1+\cos(2\omega t_1))\boldsymbol{\sigma}_x - \sin(2\omega t_1)\boldsymbol{\sigma}_y\right), \left((1+\cos(2\omega t_2))\boldsymbol{\sigma}_x - \sin(2\omega t_2)\boldsymbol{\sigma}_y\right)\right] \\
&= \frac{E(t_1)E(t_2)}{32}\Big((1+\cos(2\omega t_1))\sin(2\omega t_2)\left[\boldsymbol{\sigma}_x, \boldsymbol{\sigma}_y\right] + \sin(2\omega t_1)(1+\cos(2\omega t_2))\left[\boldsymbol{\sigma}_y, \boldsymbol{\sigma}_x\right]\Big) \\
&= i\frac{E(t_1)E(t_2)}{32}\Big((1+\cos(2\omega t_1))\sin(2\omega t_2) - \sin(2\omega t_1)(1+\cos(2\omega t_2))\Big)\boldsymbol{\sigma}_z \qquad (30) \\
&= -i\frac{E(t_1)E(t_2)}{4}\cos(\omega t_1)\cos(\omega t_2)\sin(\omega(t_1-t_2))\boldsymbol{\sigma}_z. \qquad (31)
\end{aligned}$$

A few important qualitative properties of the integrand and thus of the second order Magnus expansion term can be inferred from (31). Firstly, containing only the commutator $[\boldsymbol{\sigma}_x, \boldsymbol{\sigma}_y]$, the integrand

is proportional to $\boldsymbol{\sigma}_z$ and represents the second order "composition effect" of non-commuting rotations around different axes in the $x-y$ plane. Furthermore, for $t_1 = t_2$ the final sine factor is zero, as is to be expected for the commutator at equal times.

Noting that this integrand is to be doubly integrated over t_1 and t_2, it is wise to make the integrand separable into factors only depending on t_1 or t_2. This yields the integrand

$$\begin{aligned}
&\frac{-iE(t_1)E(t_2)}{4}\cos(\omega t_1)\cos(\omega t_2)\left(\sin(\omega t_1)\cos(\omega t_2)-\cos(\omega t_1)\sin(\omega t_2)\right)\boldsymbol{\sigma}_z \\
=&\frac{-i}{8}\boldsymbol{\sigma}_z\left(E(t_1)\sin(2\omega t_1)E(t_2)\cos(\omega t_2)^2\right)+\frac{i}{8}\boldsymbol{\sigma}_z\left(E(t_1)\cos(\omega t_1)^2E(t_2)\sin(2\omega t_2)\right). \qquad (32)
\end{aligned}$$

We proceed by performing the inner integrals over $\mathrm{d}t_2$, resulting in

$$\begin{aligned}
\int_{t_0}^{t_1}\mathrm{d}t_2\,E(t_2)\cos(\omega t_2)^2 &= \int_{t_0}^{t_1}\mathrm{d}t_2\,(E_0+E_1t_2)\cos(\omega t_2)^2 \\
&= \frac{1}{4}(t_1-t_0)\left(E(t_0)+E(t_1)\right) \\
&\quad+\frac{1}{4\omega}\left(E(t_1)\sin(2t_1\omega)-E(t_0)\sin(2t_0\omega)\right) \\
&\quad+\frac{E_1}{8\omega^2}\left(\cos(2t_1\omega)-\cos(2t_0\omega)\right) \qquad (33) \\
\int_{t_0}^{t_1}\mathrm{d}t_2\,E(t_2)\sin(2\omega t_2) &= \int_{t_0}^{t_1}\mathrm{d}t_2\,(E_0+E_1t_2)\sin(2\omega t_2) \\
&= \frac{1}{2\omega}\left(E(t_0)\cos(2t_0\omega)-E(t_1)\cos(2t_1\omega)\right) \\
&\quad+\frac{E_1}{4\omega^2}\left(\sin(2t_1\omega)-\sin(2t_0\omega)\right). \qquad (34)
\end{aligned}$$

Plugging (33) and (34) into the integral of (32) over $\mathrm{d}t_2 \in [t_0, t_1]$ yields

$$\begin{aligned}
&-\frac{i}{8}\boldsymbol{\sigma}_zE(t_1)\sin(2\omega t_1)\Big(\frac{1}{4}(t_1-t_0)\left(E(t_0)+E(t_1)\right) \\
&\qquad+\frac{1}{4\omega}\left(E(t_1)\sin(2t_1\omega)-E(t_0)\sin(2t_0\omega)\right) \\
&\qquad+\frac{E_1}{8\omega^2}\left(\cos(2t_1\omega)-\cos(2t_0\omega)\right)\Big) \\
&+\frac{i}{8}\boldsymbol{\sigma}_zE(t_1)\cos(\omega t_1)^2\Big(\frac{1}{2\omega}\left(E(t_0)\cos(2t_0\omega)-E(t_1)\cos(2t_1\omega)\right) \\
&\qquad+\frac{E_1}{4\omega^2}\left(\sin(2t_1\omega)-\sin(2t_0\omega)\right)\Big), \qquad (35)
\end{aligned}$$

which thankfully can be simplified (by Mathematica, not by me...) to

$$\begin{aligned}
&\frac{i}{16}\boldsymbol{\sigma}_zE(t_1)\cos(\omega t_1)(t_0-t_1)(E(t_0)+E(t_1))\sin(\omega t_1) \\
&-\frac{i}{16\omega}\boldsymbol{\sigma}_zE(t_1)\cos(\omega t_1)(E(t_1)\cos(\omega t_1)-E(t_0)\cos(\omega(2t_0-t_1))) \\
&+\frac{iE_1}{32\omega^2}\boldsymbol{\sigma}_zE(t_1)\cos(\omega t_1)(\sin(\omega t_1)-\sin(\omega(2t_0-t_1))). \qquad (36)
\end{aligned}$$

Finally, we calculate the second order Magnus exponent term by integrating the previous expression

with respect to $\mathrm{d}t_1$ over an evolution interval t_c, starting from t_0:

$$\begin{aligned}\frac{i}{t_c}\Omega_2(t_0+t_c,t_0) = &\frac{E(t_0)^2}{32\omega}\boldsymbol{\sigma}_z(1-2\cos(2\omega t_0)) \\ &+\frac{E_1E(t_0)}{32\omega^2}\boldsymbol{\sigma}_z\left(\pi-2\pi\cos(2\omega t_0)-3\sin(2\omega t_0)\right) \\ &+\frac{E_1^2}{384\omega^3}\boldsymbol{\sigma}_z\left(3+4\pi^2+(18-6\pi^2)\cos(2\omega t_0)+18\pi\sin(2\omega t_0)\right). \end{aligned} \tag{37}$$

Direct calculation of the second order Magnus term using Daniel's scripts yields the same expression, which is comforting.

The first term of (37) represents the Bloch-Siegert shift and is the only term that survives for a constant drive with $E_1 = 0$. For $t_0 = kt_c$, we can understand the second term and the parts of third term that contain π^2 as the increase in Bloch-Siegert shift during the evolution interval t_c, similar to (22).

Noting that the expressions and integrals become increasingly complicated for higher order Magnus terms, we stop here with the manual integration and intuitive interpretation of the Magnus terms.

References

1. W. Magnus. On the Exponential Solution of Differential Equations for a Linear Operator. *Communications on pure and applied mathematics* **7,** 649–673 (1954).
2. J. S. Waugh. in *Encyclopedia of Magnetic Resonance* (ed R. K. Harris) 00000 (John Wiley & Sons, Ltd, Chichester, UK, Mar. 15, 2007). ISBN: 978-0-470-03459-0. doi:10.1002/9780470034590.emrstm0020. http://doi.wiley.com/10.1002/9780470034590.emrstm0020 (2017).
3. S. Blanes, F. Casas, J. Oteo & J. Ros. The Magnus Expansion and Some of Its Applications. *Physics Reports* **470,** 151–238. ISSN: 03701573 (5-6 Jan. 2009).
4. S. Blanes, F. Casas, J. A. Oteo & J. Ros. A Pedagogical Approach to the Magnus Expansion. *European Journal of Physics* **31,** 907–918. ISSN: 0143-0807, 1361-6404 (July 1, 2010).